Molecular Therapy
Methods & Clinical Development
Original Article

Biocompatible, Purified *VEGF-A* mRNA Improves Cardiac Function after Intracardiac Injection 1 Week Post-myocardial Infarction in Swine

Leif Carlsson,[1,9] Jonathan C. Clarke,[2,3,9] Christopher Yen,[4,9] Francine Gregoire,[5] Tamsin Albery,[1] Martin Billger,[6] Ann-Charlotte Egnell,[1] Li-Ming Gan,[1] Karin Jennbacken,[1] Edvin Johansson,[7] Gunilla Linhardt,[1] Sofia Martinsson,[1] Muhammad Waqas Sadiq,[1] Nevin Witman,[3] Qing-Dong Wang,[1] Chien-Hsi Chen,[4] Yu-Ping Wang,[4] Susan Lin,[4] Barry Ticho,[5] Patrick C.H. Hsieh,[4,8] Kenneth R. Chien,[2,3] and Regina Fritsche-Danielson[1]

[1]Innovative Medicines and Early Development Biotech Unit, Cardiovascular, Renal and Metabolic Diseases, AstraZeneca, Mölndal 431 83, Sweden; [2]Integrated Cardiometabolic Center, Karolinska Institute, Huddinge 141 52, Sweden; [3]Department of Cell and Molecular Biology and Medicine, Karolinska Institute, Stockholm 171 77, Sweden; [4]Institute of Biomedical Sciences, Academia Sinica, Taipei 115, Taiwan; [5]Moderna Therapeutics, Cambridge, MA, USA; [6]Drug Safety and Metabolism, Regulatory Safety, Innovative Medicines and Early Development Biotech Unit, AstraZeneca, Gothenburg, Sweden; [7]Personalised Healthcare and Biomarkers, Innovative Medicines and Early Development Biotech Unit, AstraZeneca, Gothenburg, Sweden; [8]Institute of Medical Genomics and Proteomics, Institute of Clinical Medicine and Cardiovascular Surgery Division, National Taiwan University and Hospital, Taipei 100, Taiwan

mRNA can direct dose-dependent protein expression in cardiac muscle without genome integration, but to date has not been shown to improve cardiac function in a safe, clinically applicable way. Herein, we report that a purified and optimized mRNA in a biocompatible citrate-saline formulation is tissue specific, long acting, and does not stimulate an immune response. In small- and large-animal, permanent occlusion myocardial infarction models, *VEGF-A 165* mRNA improves systolic ventricular function and limits myocardial damage. Following a single administration a week post-infarction in mini pigs, left ventricular ejection fraction, inotropy, and ventricular compliance improved, border zone arteriolar and capillary density increased, and myocardial fibrosis decreased at 2 months post-treatment. Purified *VEGF-A* mRNA establishes the feasibility of improving cardiac function in the sub-acute therapeutic window and may represent a new class of therapies for ischemic injury.

INTRODUCTION

Cardiovascular disease remains a leading cause of morbidity and mortality worldwide.[1–3] To date, there has not been any significant clinically feasible and/or proven targeted biologic strategy for treating congestive heart failure.[4,5] Manipulation of the cardiac gene expression in a rapid, dosable, and tissue-specific fashion without genomic integration would represent a major advance in biologic therapies. mRNA therapy with transcripts made from naturally occurring modifications is an evolving technology that has these characteristics, and recent papers have reported improved mRNA transcripts with N1-methylpseudouridine,[6,7] as well as capping efficiency and UTR optimization.[8]

Previous studies have shown that vascular endothelial growth factor A (VEGF-A) 165 plays a critical, dominant role in the regulation of new blood vessel formation, has a pro-survival effect on vascular, endothelial, and cardiac cells, and enhances endothelial proliferation from epicardial-derived progenitor cells (for review, see Ferrara et al.[9]).[9–11] However, while a variety of approaches including plasmid DNA, viral vectors, recombinant proteins, and protein conjugates have attempted to improve cardiac function via VEGF-A 165, none of these attempts has led to clinically tractable effects.[4,12–18] Considering this, an optimal therapeutic modality that provides a tissue-restricted, safe, rapid, short-duration, and dosable therapeutic level is required. VEGF-A protein expression produced from an mRNA transcript that is highly purified, non-immunogenic, and optimized for clinical production may fulfill these requirements.

Prior *in vivo* work with modified *VEGF-A* mRNA (*VEGF* mRNA) therapies has relied on cationic lipid carriers and non-optimized mRNA transcript production methods. A lipid-based delivery system can result in infusion-related hypersensitivity reactions, can be associated with tissue injury, and can promote RNA degradation via modulation of the local innate immune system.[19–21] Zangi et al.[11] have shown that a single intra-cardiac injection of *VEGF* mRNA post-myocardial infarction (MI) can improve cardiac dysfunction and long-term survival, although the formulation included a

Received 26 March 2018; accepted 4 April 2018;
https://doi.org/10.1016/j.omtm.2018.04.003.

[9]These authors contributed equally to this work.

Correspondence: Kenneth R. Chien, Department of Cell and Molecular Biology and Medicine, Karolinska Institute, Stockholm 171 77, Sweden.
E-mail: kenneth.chien@ki.se
Correspondence: Regina Fritsche-Danielson, Innovative Medicines and Early Development Biotech Unit, Cardiovascular, Renal and Metabolic Diseases, AstraZeneca, Mölndal 431 83, Sweden.
E-mail: regina.fritsche-danielson@astrazeneca.com

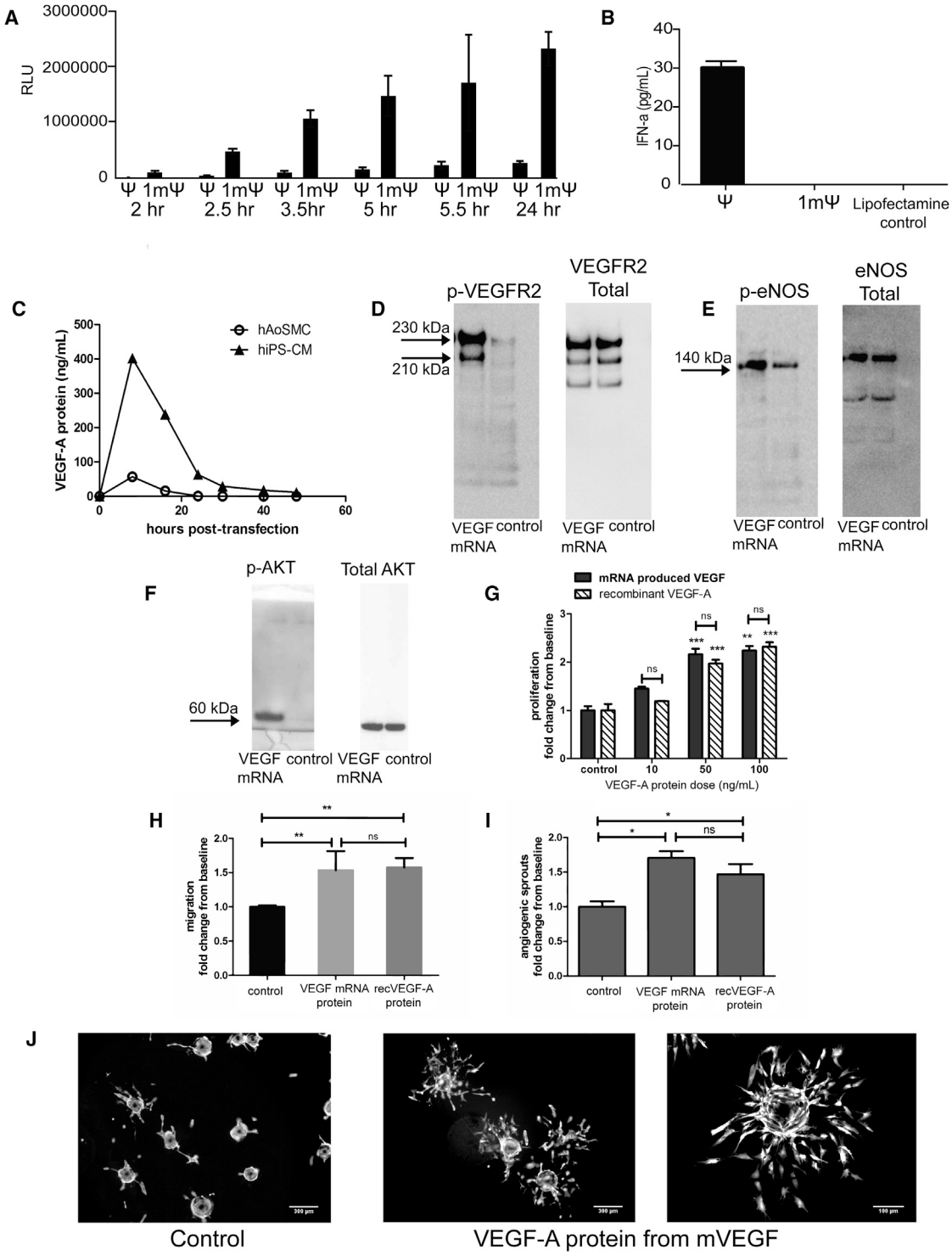

Figure 1. Optimized *VEGF-A* mRNA Produces Functional Protein *In Vitro*

(A) Purified mRNA with 1-methylpseudouridine (m1Ψ) produces higher levels of luciferase protein when compared to first generation (pseudouridine [Ψ]) in 20,000 HeLa cells with 200 ng of mRNA and (B) less innate immune reactivity measured as interferon-alpha secretion in 500,000 primary human PBMC cells after transfection with 500 ng of mRNA. (C) Time course of VEGF-A protein production in human aortic smooth muscle cells (hAoSMC) and in human iPS-derived cardiomyocytes (hiPS-CM) after transfection with purified *VEGF* mRNA, showing that relevant primary cardiac cell types can be transfected. VEGF protein transcribed from *VEGF* mRNA is biologically active and activates

(legend continued on next page)

non-optimized, primitive mRNA transcript in a lipid carrier. In addition, a recent study in small animals recently reported mRNA can be expressed in the heart without the need for lipid carriers.[7,22] Accordingly, it remains unclear whether a *VEGF* mRNA can lead to functional cardiac improvement in small and large animals.

Herein, we report a human *VEGF-A* mRNA transcript, produced and manufactured in large scale with optimized capping efficiency, UTR, and nucleotide design and purification, as described by Richner et al.,[8] which when formulated in a biocompatible buffer drives physiological endpoints without immunogenicity, not only in rat, but also in large animals. In a swine permanent ligation model, we report a dose-dependent improvement in left ventricular ejection fraction (LVEF), inotropic function and compliance, border zone capillary and arteriole density, and a reduction in myocardial fibrosis at 2 months post-treatment. Furthermore, when intradermally or intravenously administered to rat and cynomolgus monkeys, the optimized *VEGF* mRNA did not provoke any innate immune response. Taken together, these studies support a tractable *VEGF* mRNA delivery system for reparative therapy in heart, skeletal muscle, and skin via paracrine gain-of-function strategies that can be taken into the clinic.

RESULTS

Protein Produced from Purified *VEGF* mRNA Transcript Is Functionally Equivalent to Recombinant Protein *In Vitro*

In traditional molecular biology techniques, RNA transcript synthesis was originally described using the classical base pairs, adenine, uridine, guanine, and cytosine. However, there are now known to be more than 100 modifications of these bases, some of which affect transcript stability and can cause alternative folding, leading to new tertiary structures.[23–26] Early generations of mRNA transcripts with modified nucleotides, where pseudouridine (Ψ) replaced uridine, activated the innate immune system, as has been previously shown.[7,11,27,28] However, with further optimized generations, including replacement of pseudouridine with 1-methylpseudouridine (m1Ψ)[6,11] and further optimizations in purification and capping efficiency,[8] mRNA transcripts produce increased protein levels without causing an innate immune response (Figures 1A and 1B). To confirm the purified (m1Ψ) human *VEGF* mRNA transcript would translate into a secreted and functional protein, we demonstrated VEGF-A protein in mRNA-transfected human smooth muscle cells and cardiomyocytes (Figure 1C). To test downstream activation, we assayed phosphorylation of the VEGF receptor 2 (Figure 1D), endothelial nitric oxide synthase (Figure 1E), and AKT (Figure 1F), and found an increase in phosphorylated protein compared to the control.

To confirm that the protein produced from the *VEGF* mRNA was functional, we compared the same concentration of *VEGF* mRNA-produced protein to commercially available recombinant human VEGF-A protein on human umbilical vein endothelial cell (HUVEC) proliferation and found a dose-dependent and quantitatively similar increase in both cases (Figure 1G). We also saw a comparable response of cell migration (Figure 1H) and angiogenic sprouting (Figures 1I and 1J) to the equivalent dose of VEGF-A protein, 10 ng/mL.

Efficient Transfection by Citrate-Saline-Formulated mRNA in Skin, Heart, and Skeletal Muscle

The first studies using RNA as a method of gene delivery and protein overexpression injected naked RNA into both the skeletal muscle[29] and the brain.[30] However, this can trigger immune response.[24,27,31–38] More recent studies with mRNA have used a combination of liposomal delivery mechanisms as well as non-toxic buffers.[7,11,28,39,40] Based on these *in vivo* RNA studies, we screened for transfection and protein expression efficiency in multiple organs using mRNA in a citrate-saline buffer. Using this buffer, we injected mRNA encoding firefly luciferase into liver (Figure 2A), kidney (Figure 2B), pancreas (Figure 2C), heart (Figure 2D), skeletal muscle (Figure 2E), and skin (Figure 2F), revealing expression only in the skin, heart, and skeletal muscle. To test for off-target expression of luciferase outside of the heart and skeletal muscle, we prolonged the IVIS exposure time to 5 min, measured bioluminescence, and found luciferase expression only in the target organs (Figures 2D and 2E).

Not only was there tissue-specific, localized uptake in striated muscle and skin, but there also was significant long-term expression with the purified luciferase mRNA. For the skin and skeletal muscle, there was expression >216 hr (Figures 2F and 2G), and for the skeletal muscle the expression extended to >30 days (Figure 2J). In cardiac muscle, there was rapid protein expression within 30 min that peaked at 24 hr, persisted for 4 days, and was negative by day 7 (Figures 2H–2J). Peak levels at 24 hr were similar across all three organs (Figure 2I).

mRNA Localizes in Cardiac Interstitium prior to Uptake by Cardiomyocytes

Further examining the expression pattern of modified mRNA, we also demonstrated efficient *in vivo* cardiac uptake and translation of *lacZ* mRNA in citrate-saline (Figures 3A and 3B). To determine mRNA localization, we performed RNA *in situ* hybridization and assayed for VEGF-A protein up to 48 hr after intracardiac injection with probes for *VEGF-A* mRNA (Figures 3C–3L), where staining was seen throughout the myocardium of *VEGF-A* mRNA (Figure 3C) and protein (Figure 3D). Neither mRNA (Figure 3E) nor VEGF-A protein (Figure 3F) was detected in the citrate-saline-injected control animals.

VEGFR2 and downstream signaling pathways, shown by phosphorylation of (D) VEGF-Receptor 2 in human endothelial cells (HUVECs), (E) endothelial nitric oxide synthase in HUVECs, and (F) AKT in mouse cardiac fibroblasts cells in culture (representative western blot images shown; n = 2). (G) VEGF-A protein produced from *VEGF* mRNA and recombinant VEGF-A (recVEGF-A) induce similar responses and increase endothelial cell proliferation (n = 3). (H) Endothelial cell migration (n = 2; VEGF-A dose: 10 ng/mL) and (I) angiogenic sprouting in endothelial cells (n = 3; VEGF-A dose: 10 ng/mL) compared to controls. (J) Representative images on angiogenic sprouting in control cells and cells stimulated with VEGF-A protein produced from *VEGF* mRNA. Data are presented as mean ± SEM. Control is medium only without VEGF-A protein. Asterisks represent: *$p < 0.05$ versus control; **$p < 0.01$ versus control; ***$p < 0.001$ versus control.

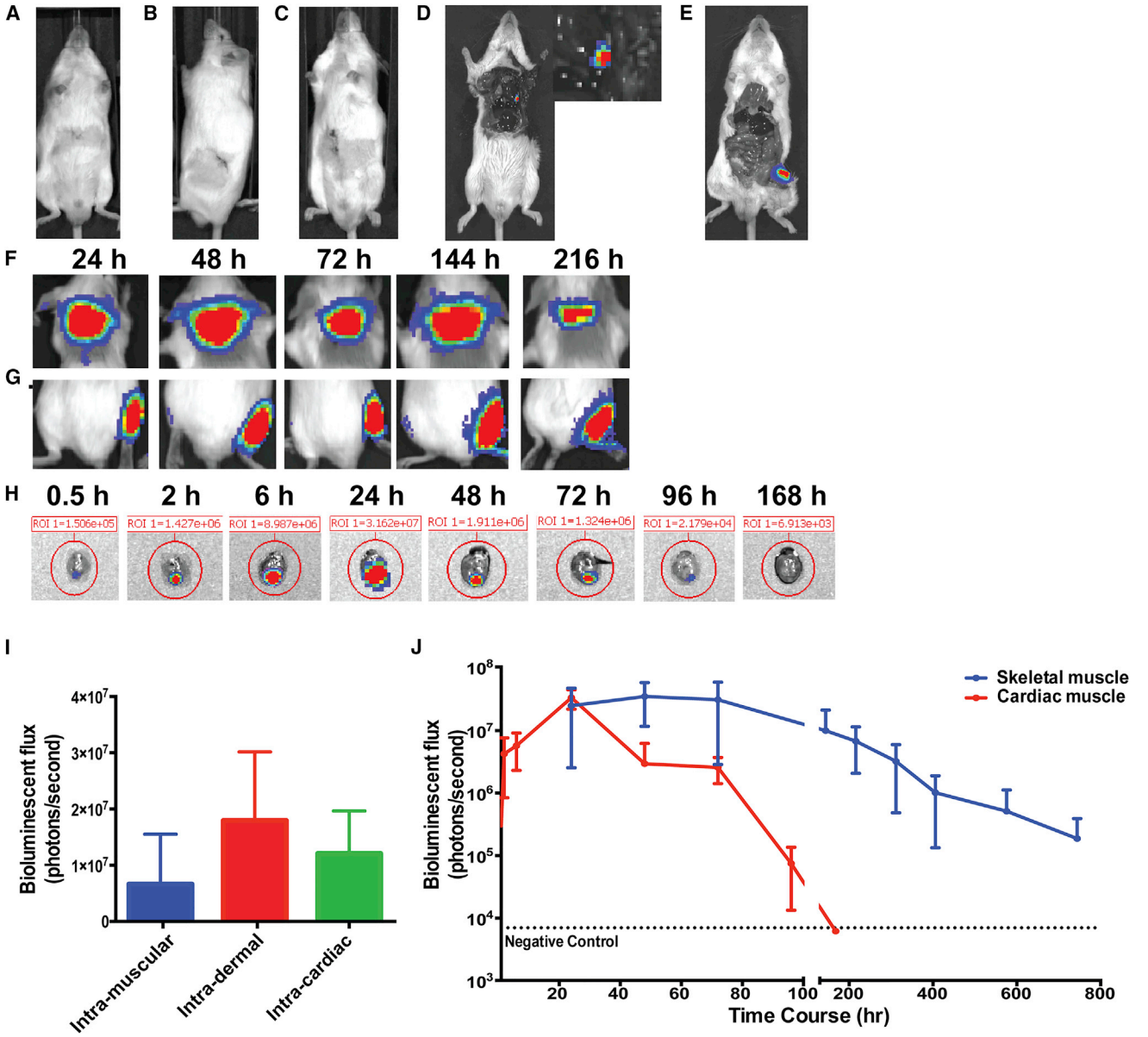

Figure 2. Injections of Luciferase mRNA in a Biologically Compatible Citrate-Saline Formulation Produces Luciferase in the Skin, Skeletal Muscle, and Heart

To test for *in vivo* protein expression without a lipid carrier, 25 μg of citrate-saline (cs) formulated mRNA encoding for firefly luciferase was injected into the (A) liver, (B) kidney, (C) pancreas, (D) heart, and (E) skeletal muscle and assayed for protein with IVIS camera 24 hr after injection as shown in representative images. 15 μg of purified cs-luciferase mRNA was injected into the (F) dermis, (G) skeletal muscle, and (H) cardiac muscle. Representative images at different time points over 9 days are shown. (I) Comparative expression of luciferase in the dermis, skeletal muscle, and heart at 24 hr. (J) Long-term luciferase expression in cardiac and skeletal muscle injected with 15 μg purified cs-luciferase mRNA. n = 3 for all experiments. Data are presented as mean ± SEM.

Co-staining of *VEGF* mRNA *in situ* hybridization with Troponin antibody showed co-localization in cardiomyocytes (Figure 3G). Within 1 hr, there was heterogeneous cell uptake of mRNA and protein production (Figure 3H) where mRNA could be seen along the cardiomyocyte cell membrane (Figure 3H, arrow). At 3–24 hr, *VEGF* mRNA and protein were further seen in the intracellular compartment (Figures 3I–3K), and initial degradation products by 48 hr (Figure 3L).

Human *VEGF* mRNA Transfection Is Saturable and Improves Cardiac Function

To quantify protein production from purified citrate saline (cs)-*VEGF* mRNA and to find a comparable dose to cationic lipid-formulated mRNA, we injected 150 μg of cs-*VEGF* mRNA and 100 μg of *VEGF* mRNA in RNAiMax into the mouse heart. After 24 hr, VEGF-A protein levels and the pharmacokinetic profiles in

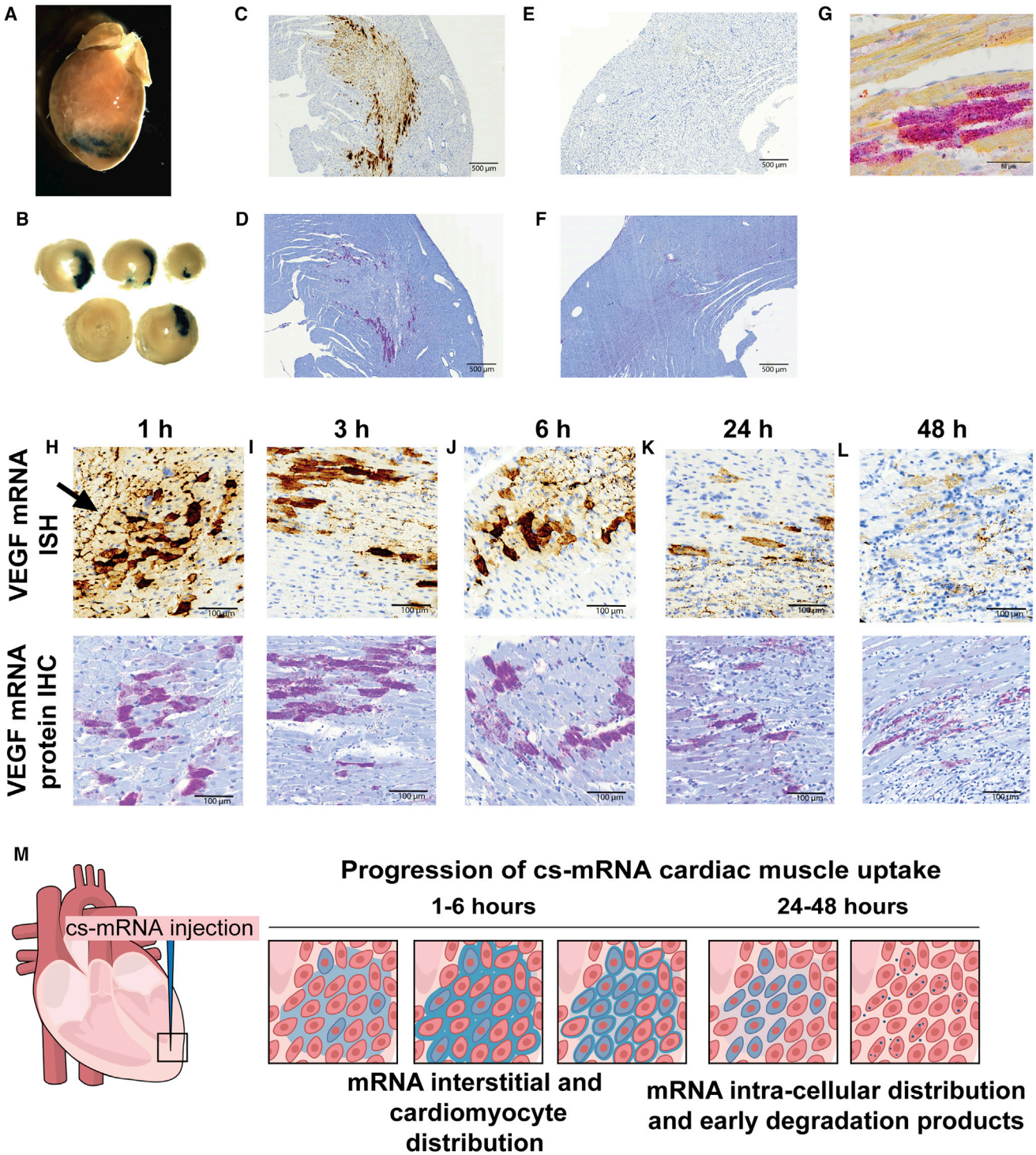

Figure 3. *LacZ* and VEGF mRNA Cardiac Transfection and Translation in Biologically Compatible Citrate-Saline Buffer (cs-mRNA)

(A and B) 75 µg of *lacZ* mRNA was injected into the mouse heart and whole mount stained with X-gal after 48 hr. *In situ* (C and E) and immunohistochemistry (D and F) of 100 µg *VEGF* mRNA (C and D) intracardiac injection in rats and citrate-saline control (E and F). (G) Co-staining of troponin T and VEGF-A protein with immunohistochemistry showed that the injected *VEGF* mRNA was taken up and translated by cardiomyocytes. *VEGF* mRNA and protein expression were followed by *in situ* hybridization and immunohistochemistry 1 (H), 3 (I), 6 (J), 24 (K), and 48 (L) hr after intracardiac injection of 100 µg VEGF mRNA. (H) Arrow highlighting interstitial *VEGF* mRNA localization. (M) Cartoon representation of mRNA cardiac uptake.

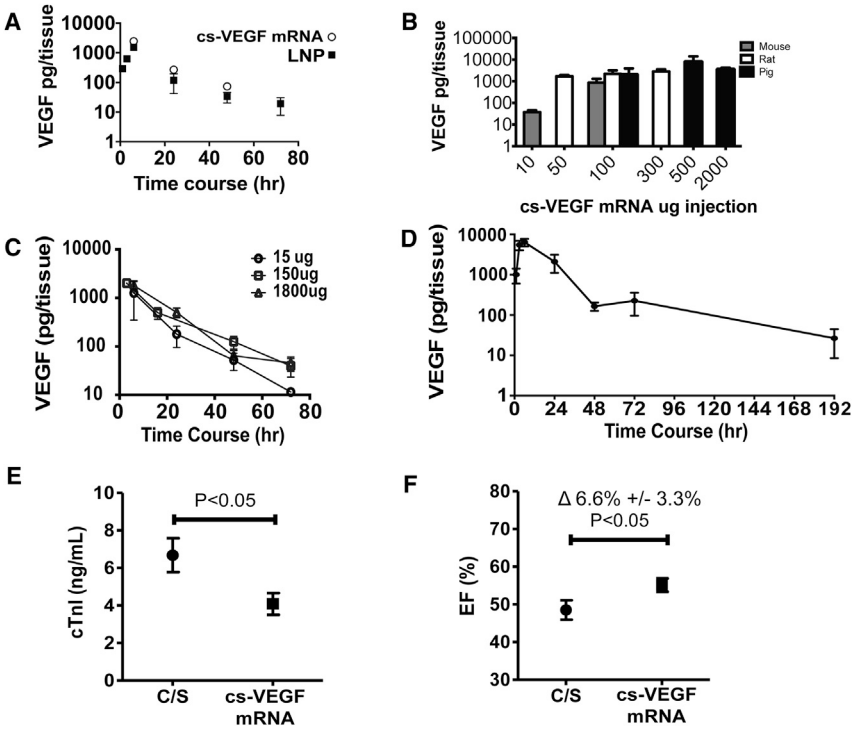

Figure 4. VEGF-A Protein Pharmacokinetics and Effect on Cardiac Troponin I Release and Left Ventricular Function Post-myocardial Infarction following Intracardiac Injection of Purified *VEGF* mRNA in a Biologically Compatible Citrate-Saline Formulation (cs-*VEGF* mRNA)

(A) VEGF-A protein pharmacokinetics after single cardiac injections of cs-*VEGF* mRNA versus RNAiMax (lipid nanoparticle [LNP]) in the mouse over 72 hr (n = 3 per time point and formulation). (B) Cross-species comparison of VEGF-A protein levels following increasing intracardiac dosing of cs-*VEGF* mRNA (n = 3–4 for each dose and species). (C) Pharmacokinetics of VEGF-A protein produced by increasing intracardiac doses, 15, 150, and 1,800 μg, of cs-*VEGF* mRNA (n = 3 per time point and dose) in the rat. (D) 100 μg of cs-*VEGF* mRNA expressed up to 192 hr (n = 3 per time point). (E) Circulating cardiac troponin I (cTnI) levels at day 1 following permanent occlusion of the left anterior descending coronary artery to induce MI in the rat. Citrate-saline vehicle (C/S, n = 8) or cs-*VEGF* mRNA (150 and 1,800 μg dose groups pooled; n = 19) was intracardially injected at the time of the induction of the MI. (F) Left ventricular ejection fraction (EF), assessed by cardiac magnetic resonance imaging 8 days after the occlusion of the coronary artery. Data are means ± SEM.

cs-*VEGF* mRNA-injected hearts were comparable to mice injected with lipid carrier-*VEGF* mRNA (Figure 4A). Interestingly, we found that the protein expression was dose limited and saturable across species (Figure 4B), and in the rat a 10-fold increase in dose increased the area under the curve by 1.6-fold only (Figure S1). Three single doses, 15, 150, and 1,800 μg, were further examined in the rat heart, and all gave rise to similar peak protein levels and pharmacokinetic profiles (Figure 4C). VEGF-A protein was seen out to 190 hr in the rat heart (Figure 4D), comparable to previous studies of mRNA-derived protein.[7]

Knowing that Zangi et al.[11] showed an early beneficial effect post-MI by day 8, we tested the degree of ventricular functional improvement with the optimized cs-*VEGF* mRNA in rats subjected to permanent occlusion of the left anterior descending coronary artery. Indeed, pooling included animals from the two dose groups (150 and 1,800 μg) because the purified *VEGF* mRNA injected produced similar amounts of VEGF-A protein and showed cardiac troponin I levels to be significantly lower day 1 post-MI (Figure 4E). At study termination day 8 post-MI, LVEF was significantly increased by 6.6% ± 3.1% ($p < 0.05$) in the VEGF mRNA group versus citrate-saline (Figure 4F).

VEGF mRNA Improves Swine Cardiac Function when Given 1 Week Post-MI

We next investigated whether purified cs-*VEGF* mRNA could demonstrate therapeutic potential in a swine permanent ligation model of MI when delivered in the sub-acute phase (Figures 5A and 5B). One of two doses (1 mg: cs-*VEGF* mRNA L or 10 mg: cs-*VEGF* mRNA H) of purified cs-*VEGF* mRNA or citrate-saline vehicle was delivered via intracardiac injections across the peri-infarct and infarct area at 7 days after induction of MI (Figure 5B). To monitor changes in cardiac function, we carried out serial echocardiographic examinations over the course of the study, in conjunction with pressure-volume (PV) loop measurement prior to sacrifice at 2 months post-injections (Figures 5C and 5D).

Two months after injections, we observed significant improvements across several cardiac systolic parameters. Echocardiographic measurements showed that at 2 months post-treatment, pigs in both the cs-*VEGF* mRNA L and cs-*VEGF* mRNA H groups demonstrated significant improvements in LVEF compared to the citrate-saline vehicle group, as well as their respective day 7 readouts (Figure 5C). LVEF recovered to 51% ± 0.9% in the cs-*VEGF* mRNA L group and 52 ± 1.0% in the cs-*VEGF* mRNA H group, whereas in the vehicle group no such recovery was observed with LVEF remaining at 47% ± 0.8% (Figure 5C).

Improvement in cardiac systolic function and contractility was further corroborated by invasive hemodynamic assessments via PV loop, which showed significant improvements across several systolic function parameters, such as the rate of pressure development (dp/dt max) and left ventricular end systolic pressure (LVESP), as well as load-independent variables upon performing occlusions such as end-systolic PV relationship (ESPVR) and preload recruitable stroke work (PRSW) (Figures 5E–5H). Furthermore, there was a statistically

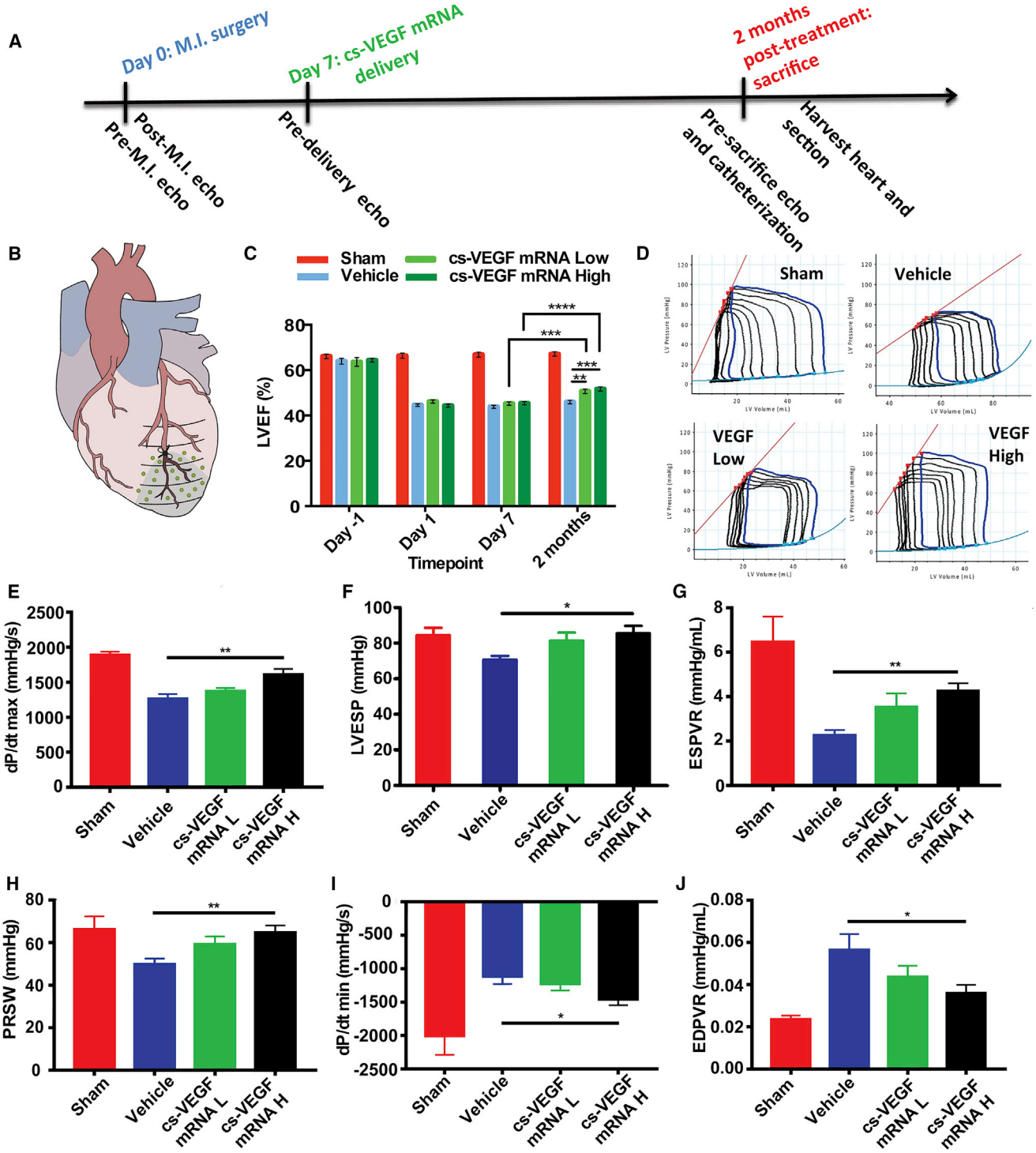

Figure 5. Effects of Intracardiac Purified cs-*VEGF* mRNA or Citrate-Saline Vehicle Injection 7 Days after Myocardial Infarction on Cardiac Function

(A) Timeline of intracardiac injections of citrate-saline (vehicle), 1 mg cs-*VEGF* mRNA L, and 10 mg cs-*VEGF* mRNA H. (B) Cartoon representation of injection sites in green dots. (C) Left ventricular ejection fraction (LVEF) as measured by echocardiography before and after MI (day 0), 1 week after MI before injections (day 7), and 2 months after

(legend continued on next page)

significant improvement in the high-dose group in myocardial compliance, including the rate of myocardial relaxation (dp/dt min) (Figure 5I) and end-diastolic PV relationship (EDPVR) (Figure 5J).

VEGF mRNA Increases Vessel Density in the Peri-infarct Area and Decreases Myocardial Fibrosis

Upon termination of the experiment at 2 months post-treatment, the heart was harvested and sectioned into 10- to 15-mm slices to measure infarct size (IS) (Figure 6A). The myocardial tissue was then stained to assess vessel density in the peri-infarct region, and extent of interstitial fibrosis in samples taken remote from the infarct region (Figure 6B). IS was measured according to previously published methods in this type of animal model[41–44] and was associated with *VEGF* mRNA treatment (Figures 6C and 6D), with the significant reduction being seen in the mid-ventricular slice, corresponding approximately to the site of permanent LAD occlusion (cs-*VEGF* mRNA L: 3.4% ± 1.7%; cs-*VEGF* mRNA H: 2.2% ± 1.1%; vehicle: 8.2% ± 1.7%; Figures 6E and 6F). Analysis of the peri-infarct zone using immunofluorescence staining of isolectin-b4 and SM-22α revealed marked neovascularization upon cs-*VEGF* mRNA treatment, with increases in both capillary (Figure 6G) and arteriole density (Figure 6H). Additionally, Masson trichrome staining for collagen deposition in the myocardium remote from the infarct zone indicated a decreased magnitude of fibrosis in the cs-*VEGF* mRNA-treated pigs as compared to vehicle-injected pigs (Figure 6I). Taken together, these results suggest that the purified *VEGF* mRNA injected 1 week after permanent left anterior descending (LAD) occlusion improves systolic function, increases long-term vessel density in the peri-infarct area, and attenuates infarct expansion and remote fibrosis.

VEGF mRNA Does Not Activate the Innate Immune System When Intradermally or Intravenously Injected in Cynomolgus Monkeys or Rats

In male cynomolgus monkeys (n = 4/group), intradermal (0.5–3 mg/animal) or intravenous (3 mg/animal) injection of *VEGF* mRNA was not associated with any treatment-related increases in IL-6 or IL-8 as assessed 3, 6, and 24 hr after administration. Hence, in all animals, at all doses of *VEGF* mRNA (or citrate-saline vehicle) and all time points the levels of IL-6 were below the lower limit of quantification for the assay (8.40 pg/mL; Table S1). For IL-8, the plasma levels in samples from *VEGF* mRNA-treated animals did not differ versus the levels seen in the vehicle-treated animals at any dose level or sampling time point.

In the male rat (n = 10/group), intradermal doses were not associated with any measurable increases of IL-6 or keratinocyte-derived chemokine (KC). All males administered 3 mg/animal by the intravenous route had measurable levels of KC at the 3-hr time point on day 1. By 24 hr after dosing, all KC values were below the lower limit of quantification (Table S2). Given the incidence and magnitude of the values noted, this was not considered to be related to treatment with *VEGF* mRNA.

DISCUSSION

The ability to regulate the genetic program of solid organs in a rapid-onset, biocompatible, and tissue-specific manner could offer new approaches for life-threatening forms of acute organ injury. Purified mRNA in a biologically compatible formulation has these abilities. Compared to DNA vector systems that lead to permanent expression and angioma formation[45] and recombinant VEGF-A protein, which has a short half-life, the pharmacokinetics of *VEGF* mRNA is an attractive alternative.[46]

VEGF-A pathways play a central role in the control of cardiovascular physiological function in general and angiogenesis in particular. Roles include activation of anti-apoptotic pathways,[47] nitric oxide (NO) signaling,[48] vascular permeability,[49] tumor angiogenesis,[50,51] arteriogenesis,[52] endothelial replication,[53] and as a cell fate switch for multipotent cardiovascular progenitors.[10] While inhibition of *VEGF-A* pathways has become standard of care in selected forms of cancer[54] and macular degeneration,[55] it has remained challenging to unlock the potential of augmenting *VEGF-A* pathways for potential therapeutic effects.

While earlier studies have attempted to use VEGF for cardiovascular therapy, they have been limited by side effects and rapid loss of the protein in the bloodstream.[42] Other methods to produce a functional effect of VEGF protein have been tried as well, including viral encapsulated and naked *VEGF-A* DNA plasmids, adenoviral vectors, and mRNA with a liposomal delivery mechanism.[4,11–18] However, each of these approaches has its limitations, such as limited temporal control of protein production, activation of the innate immune system, and labile protein expression. As a result, these limitations have hindered the clinical applicability of VEGF-A as a therapeutic platform for cardiovascular disease.

Previously, liposomal delivery mechanisms have been investigated as the oligonucleotide carrier system of choice. However, while lipid carriers are excellent for clinical intravenous delivery to the liver, early attempts to reach therapeutic levels of RNAi therapy in other organs have resulted in infusion-related hypersensitivity reactions, as well as hepatotoxicity, thus potentially limiting their use in other organs.[19] Hence, most clinical studies with mRNA have been hampered by their need for these carriers.[56] Recent papers have started to investigate mRNA transfection in small animals using a biocompatible carrier, but using a non-optimized transcript.[7,30,39] In this translational therapeutic paper, we build on those studies using a refined *VEGF* mRNA transcript, with capping efficiency, UTR sequence, and purification

injections. Data are means ± SEM (n ≤ 5). *p < 0.05; **p < 0.01; ***p < 0.001; ****p < 0.0001 (two-way ANOVA with Tukey's post hoc test). (D) Representative pressure-volume loops upon preload charging. Invasive hemodynamic parameter results for (E) dp/dt max, (F) LVESP, (G) ESPVR, (H) PRSW, (I) dp/dt min, and (J) EPDVR. For (D)–(J), data are means ± SEM (n ≤ 5). *p < 0.05; **p < 0.01; ***p < 0.01 (one-way ANOVA with Dunnett's post hoc test). Sham: n = 5 except EDPVR (n = 3). Vehicle: n = 8 (B and D), n = 7 (E–G), n = 6 (H and I). cs-VEGF mRNA L: n = 8 (D), n = 7 (B, E–G), n = 6 (H and I). cs-*VEGF* mRNA H: n = 8.

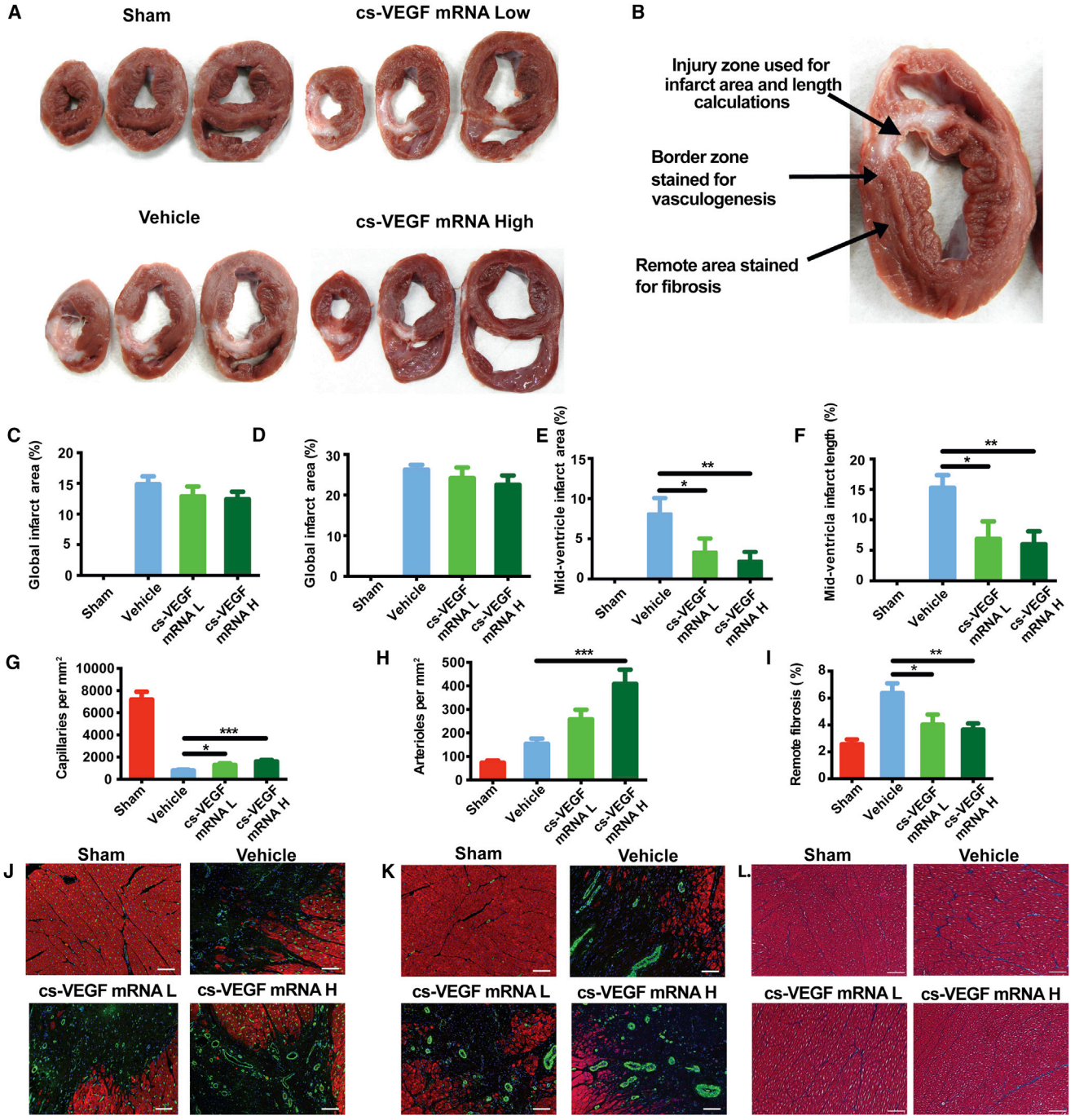

Figure 6. Effects of Intracardiac Purified cs-VEGF mRNA or Citrate-Saline Vehicle Injection 7 Days after Myocardial Infarction on Infarct and Tissue Pathophysiology Assessed 2 Months after Injection

(A) Representative slices encompassing *VEGF* mRNA injection sites processed immediately after harvesting the heart. (B) Schematic of tissue sampling regions used for downstream analyses. (C) Global infarct area. (D) Global infarct length. (E) Mid-ventricular infarct area. (F) Mid-ventricular infarct length. Quantification of (G) capillary growth, (H) arteriole growth, and (I) remote fibrosis. Representative images of each study arm for (J) isolectin-b4 (GFP)/Troponin (RFP) for angiogenesis assay, (K) SM-22α (GFP)/Troponin (RFP) staining for arteriogenesis assay, and (L) Masson Trichrome staining for remote fibrosis assay. Vehicle, cs-*VEGF* mRNA L, and cs-*VEGF* mRNA H represent citrate-saline, 1 mg cs-*VEGF* mRNA, and 10 mg cs-*VEGF* mRNA, respectively. Data are means ± SEM ($n \leq 5$). *$p < 0.05$; **$p < 0.01$; ***$p < 0.01$ (one-way ANOVA with Dunnett's post hoc test). All scale bars: 50 μm. Sham: n = 5. Vehicle: n = 8 (C–F), n = 7 (H, J, and L). cs-*VEGF* mRNA L: n = 7. cs-*VEGF* mRNA H: n = 8.

further developed for clinical translatability in a citrate-saline buffer that does not provoke innate immunity.

Interestingly, while RNA is rapidly degraded in the bloodstream within minutes, when directly injected into the myocardium, we saw prolonged VEGF protein levels. Indeed, with *VEGF* mRNA cardiac injections, at both 10 and 100 μg at 6 and 24 hr (in mouse and rat), the systemic exposure of human VEGF-A protein never was above the lower limit of quantification for the assay (data not shown), likely from RNase exposure. The cause of this prolonged duration of protein, we hypothesize, is based on a combination of factors. First, when directly injected into the heart, the mRNA will remain tissue specific and initially is seen in both intra-cardiomyocytes, but also organized along the cardiac sarcolemma, potentially acting as a protected reservoir of *VEGF* mRNA (Figure 3M). Second and in line with previous findings, we observed the uptake of the mRNA to be a saturable process with the production of the VEGF-A protein to be almost linear over a wide range of mRNA doses.[7,11] To the best of our knowledge, a clear explanation for such saturation is still lacking. Although the cellular mRNA uptake per se has been suggested to be nucleic acid specific, receptor mediated, and ion and energy dependent, other mechanisms including translation and secretion may contribute to the apparent saturation in protein production observed.[39,57] Third, when compared to VEGF protein production in previous studies,[7,11] a non-lipid-based carrier may also prolong *VEGF* mRNA protein expression, potentially because of avoidance of the local pro-inflammatory effects of lipid carriers and the interaction between a lipid-based delivery system and IFN-1 leading to more rapid mRNA clearance.[21] In addition, lipid carriers also may cause local cell necrosis, autophagy, local inflammation, and oxidative damage, and activate local apoptotic pathways.[58] This combination of interstitial localization acting as a protective reservoir, away from RNases found in the bloodstream, a saturable, active uptake mechanism, acting as a control on mRNA cellular uptake, and the use of a non-toxic carrier may allow for the prolonged expression and the consequential functional improvements in a large-animal MI model.

The mainstays of post-MI therapy are revascularization in the acute setting and neurohormonal blockade combined with blood pressure control in the acute and sub-acute window (Table S3). Our findings suggest that purified VEGF mRNA has the unique ability to combine the targets of these treatment modalities, i.e., increased blood supply, decreased cardiac fibrosis, and increased cardiac function, in a neurohormonal-independent manner that can be administered during the sub-acute time window after an MI.

In this study, MI was induced via permanent LAD ligation resulting in a chronic, non-reperfused infarct. This is in contrast to an ischemia-reperfusion model of MI in which blood flow is restored before the entire ischemic area becomes irreversibly damaged, thus enabling the salvage of a proportion of the ischemic area depending on length of ischemia. Clinically, a permanent MI model is analogous to patients in which timely and/or successful reperfusion is not achieved, whereas an ischemia-reperfusion model represents the conventional patient in whom timely PCI is performed. While a reperfusion model may be more applicable to everyday clinical practice, experimentally the permanent LAD occlusion model is a more stringent screen for therapeutic effectiveness given the severity, extent, and completeness of the infarction as compared to an ischemia-reperfusion model. However, even in this infarction model, there is improvement in the cardiac systolic function and contractility with associated increase in peri-infarct vessel density and less remote fibrosis after 2 months, suggesting the effect is long term. While the injections were given throughout the peri-infarct and infarcted tissue, the largest effect of the *VEGF* mRNA was seen in the mid-ventricular zone with the largest decrease of infarct area and increased vascularization. This is in line with our hypothesis that the mRNA will have its greatest protective effect in at-risk areas where viable cells can take up and translate the VEGF-A protein. In addition, protection of cardiomyocytes at the border zone limits further infarct expansion and preservation of healthy myocardium over time, leading to increased systolic function and contractility as indicated by echocardiography and PV loop analysis.

The data generated in this present study demonstrate a novel, refined *VEGF* mRNA transcript that has been optimized for transcript nucleotide selection,[6] UTR sequence, capping efficiency, and purification;[8] does not stimulate innate immune reaction in large animals; has prolonged expression up to 192 hr; and can limit cardiac infarct expansion and fibrosis with resulting improvement in systolic function when administered 1 week post-MI, thereby expanding the therapeutic time window from immediately after initial MI[11] to 1 week later for mRNA therapy. These results have supported the development of mRNA therapies in general and cardiac ischemia in specific, leading to a first-time-in-human ever study with *VEGF-A* mRNA, which has just been completed (ClinicalTrials.gov Identifier NCT02935712). The study was carried out in patients with type 2 diabetes mellitus primarily to assess the safety and tolerability of the mRNA given intradermally, but also included pharmacodynamic endpoints. The study is currently being reported and data will be disclosed elsewhere.

MATERIALS AND METHODS

Study Design

The research objective of this study was to investigate the potential therapeutic use of a modified and optimized *VEGF* mRNA for ischemic heart disease. The studies were conducted with small and large animals of ischemic heart failure to evaluate the effect of *VEGF* mRNA on cardiac function and assayed using imaging and interventional techniques. Power calculations were not performed to determine sample size. There were no pre-specific inclusion or exclusion criteria. All animals were randomized to treatment. No animals were excluded from the small-animal cohorts. From the large-animal studies, some exclusions were made based on anomalous recovery (complete lack of infarct) or for technical reasons. Investigators were blinded to *VEGF* mRNA post-MI treatments and outcome assessments.

mRNA Synthesis and Formulation

mRNA was synthesized *in vitro* by T7 RNA polymerase-mediated transcription from a linearized DNA template, which incorporates the 5′ and 3′ UTRs (5′ UTR-GGGAAAUAAGAGAGAAAAGAAG AGUAAGAAGAAAUAUAAGAGCCACC and 3′ UTR-UGAUAA UAGGCUGGAGCCUCGGUGGCCAUGCUUCUUGCCCCUUGG GCCUCCCCCCCAGCCCCUCCUCCCCUUCCUGCACCCGUACC CCCGUGGUCUUUGAAUAAAGUCUGA) and a poly-A tail as previously described.[8] A donor methyl group S-adenosylmethionine (SAM) was added to the methylated capped RNA (cap 0), resulting in a cap 1 structure (N7mGpppGm) to increase mRNA translation efficiency. After purification, the mRNA was diluted in citrate buffer to the desired concentration. In pseudouridine (Ψ) mRNA, cytidine and uridine were fully replaced by 5-methylcytidine and pseudouridine, respectively, and in 1 mΨ mRNA, uridine was fully replaced by N1-methylpseudouridine (see Table S4 for sequence).

In Vitro Protein Assay of Purified Luciferase mRNA and IFN Assay

To determine protein expression of purified mRNA compared to earlier formulations (pseudouridine [Ψ] versus m1Ψ), we seeded 20,000 HeLa cells (ATCC, Manassas, VA, USA) in a 96-well cell culture plate. The cells were transfected with 200 ng/well of purified luciferase mRNA using Lipofectamine 2000 (Thermo Fisher Scientific, Carlsbad, CA, USA). On the following day, the levels of firefly luciferase activity were measured using Rapid Detection of Firefly Luciferase Activity per manufacturer's instructions (Promega, Madison, WI, USA).

For investigating activation of innate immunity of the purified mRNA compared with earlier formulations, 500,000 primary human peripheral blood mononuclear cells (PBMCs; STEMCELL Technologies, Vancouver, BC, Canada) were seeded in a 96-well cell culture plate. On the next day, the cells were transfected with 500 ng/well of the purified luciferase RNA. The levels of IFN were measured using human IFN Alpha ELISA Kit per manufacturer's instructions (R&D Systems, Minneapolis, MN, USA).

Transfection of *VEGF* mRNA and Preparation of Conditioned Media

For investigating the time profile of VEGF-A protein production after mRNA transfection, 10,000 human aortic smooth muscle cells (hAoSMCs) (Lonza, Basel, Switzerland) or 20,000 human cardiomyocytes derived from induced pluripotent cells (hiPS-CMs) (Cellular Dynamics, Madison, WI, USA) were seeded into 96-well plates in smooth muscle cell basal medium supplemented with growth factors (SmGM-2) (Lonza) or fully supplemented cardiomyocyte maintenance medium (Cellular Dynamics), respectively. For preparing conditioned media containing mRNA-produced VEGF-A protein, 250,000 HUVECs (Lonza, Basel, Switzerland) were seeded in six-well plates in endothelial growth medium (EGM) (Lonza). The next day, *VEGF-A* mRNA was mixed with Lipofectamine 2000 (Invitrogen, Carlsbad, CA, USA) according to the manufacturer's instructions and added to fresh, serum-free media. After 4 hr, the transfection medium was replaced by serum-free medium, collected at specified time points, and kept at −80°C. All cell lines tested negative for mycoplasma.

ELISA for Human VEGF-A Protein

Human VEGF-A protein from conditioned media was measured with a human VEGF-A ELISA kit (Novex; Invitrogen) according to the manufacturer's instructions. Absorbance was read at 450 nm in a SpectraMax reader.

Activation of VEGF Receptor 2 Downstream Signaling by Recombinant and Purified *VEGF* mRNA Produced VEGF-A Protein

100,000 HUVECs were seeded into 12-well plates in EGM. The next day, cells were starved for 24 hr in endothelial basal medium (EBM) and then exposed to 100 ng/mL VEGF-A, either recombinant (R&D Systems, Minneapolis, MN, USA) or protein from purified *VEGF* mRNA (added as conditioned media), or to control media. Stimulation was terminated after 2, 10, and 20 min, and total protein was prepared from cultured cells with lysis buffer containing protease and phosphatase inhibitors (Mesoscale Discovery, Rockville, MD, USA). Protein concentrations were measured using the BCA Protein Assay kit (Pierce, Rockford, IL, USA).

Western Blot

Fifteen micrograms of reduced protein was loaded on a 4–12% Bis-Tris gradient gel, and electrophoresis was carried out using MES SDS running buffer (Invitrogen). Fractionated protein was electroblotted onto a polyvinyl difluoride (PVDF) membrane (Invitrogen). Membranes were blocked in 5% BSA in TBS-Tween (0.1%) and incubated with primary antibodies at 4°C overnight. Primary antibodies used were against VEGF Receptor 2 (VEGFR2), phosphorylated VEGFR2 (p-VEGFR2), AKT, phosphorylated AKT (p-AKT), endothelial nitric oxide synthase (eNOS; all from Cell Signaling, Danvers, MA, USA), and phosphorylated eNOS (p-eNOS; BD Biosciences, Franklin Lakes, NJ, USA). Membranes were incubated with a horseradish-peroxidase-labeled secondary antibody (Dako, Glostrup, Denmark), and immunoreactions were detected using the ECL western blotting substrate (Pierce). Chemiluminescent signals were visualized using a ChemiDoc Touch Imaging System (BioRad, Hercules, CA, USA).

Proliferation Assay

HUVECs were seeded in 96-well plates, at a density of 3,000 cells per well, in EGM (Lonza). The next day, medium was changed to basal EBM supplemented with 2% fetal bovine serum (FBS) with recombinant VEGF-A (R&D Systems) or to conditioned medium containing VEGF-A protein from purified VEGF mRNA. After 48 hr, cells were fixed in 4% buffered formaldehyde (Histolab, Göteborg, Sweden) and nuclei stained with Hoechst (Invitrogen) for 10 min. Fluorescent microscopy images were taken using an automated microscope (ImageXpress Micro XLS; Molecular Devices), and nuclear count was analyzed using MetaXpress software (5.3.0.1; Molecular Devices).

Migration Assay

HUVECs were stained with Cell Tracker Red (Molecular Probes, Eugene, OR, USA) according to the manufacturer's instruction and seeded in EBM supplemented with 2% FBS in transwell inserts with a FloroBlok membrane with 8-μm pore size in a 24-well plate (Corning, NY, USA). Recombinant VEGF-A (R&D Systems) or conditioned medium containing VEGF-A protein from purified *VEGF* mRNA (10 ng/mL) in EBM with 2% serum was added to the lower chamber as chemoattractant. After 24 hr, fluorescent microscopy images were obtained.

In Vitro Angiogenesis Assay

HUVECs were mixed with Cytodex 3 microcarrier beads (GE Healthcare, Little Chalfont, UK), and after 4 hr, beads coated with endothelial cells were seeded in flasks and kept at 37°C and 5% CO_2 overnight. Beads were suspended at 500 beads/mL in a fibrinogen solution (2 mg/mL; Sigma-Aldrich, St. Louis, MO, USA) containing aprotinin (0.15 U/mL; Sigma-Aldrich) and then added to wells containing thrombin (0.625 U/mL; Sigma-Aldrich) in 96-well plates. VEGF-A or conditioned medium containing VEGF-A protein from purified *VEGF* mRNA, at a concentration of 10 ng/mL, was added to the wells. As a control, medium without VEGF-A was used. Plates were kept at 37°C and 5% CO_2 for 2 days when angiogenic sprout formation was evaluated. Cells were stained with calcein for 30 min, and wide-field fluorescence images from four sites in each well were created using an automated microscope (ImageXpress XL; Molecular Devices) fitted with a 4x S fluor 0.13 NA objective (Nikon). Automated image processing and quantification was performed using a custom analysis script (MetaXpress ver. 2.7.1; Molecular Devices). Individual beads and associated cells were identified and following masking of the bead itself, cell-associated fluorescence radiating outward from the bead was quantified using measurements of intensity, length, distance, stained area, and morphology. For simplicity, stained area measurements are reported here. A Yokogawa CV7000S fitted with ×20 and ×40 objectives (Olympus UPLSAPO, 0.75 and 0.95 NA respectively) was also used to obtain maximum projection images of confocal z stacks.

Small-Animal mRNA Animal Procedures

All experiments were carried out according to European Community Council Directives and approved by Stockholm's Norra Djurförsöketiska Nämnd (Stockholm, Sweden) Göteborgs Djurförsöksetiska Nämnd (Göteborg, Sweden) and the Moderna Therapeutics Institutional Animal Care and Use Committee (Cambridge, MA, USA).

Ten- to 13-week-old male NMRI and C57/Bl6 mice, 16- to 20-week-old BALB/c female mice, and male Sprague-Dawley rats (body weight 250–300 g) were used. The animals were anesthetized with 2%–3% isoflurane and given carprofen 5 mg/kg (mice) or Marcaine (25 mg/kg) and buprenorphine (0.05 mg/kg) (rats) for analgesia. *LacZ*, luciferase, or *VEGF* mRNA was formulated in a citrate-saline biologically compatible buffer (10 mmol/L citrate, 130 mmol/L sodium chloride in Hyclone water, pH adjusted to approximately 7.5 with sodium hydroxide) or lipofectamine (Thermo Fisher Scientific, NY, USA). For cardiac injections, the left thoracic region was shaved and sterilized, and following intubation the heart was exposed through a left thoracotomy. mRNA in citrate-saline or vehicle was administered as a single injection in the left ventricular free wall in mice (50 μL total volume) and as six separate injections (15 μL each) along a line in the left ventricular free wall in the rat. In the rat MI model, the injections were given immediately following a permanent ligation of the left anterior descending coronary artery. The entire injection volume was delivered as six separate epicardial injections along the border zone of the infarct. After the injections, the thorax and the skin were closed by suturing, and excess air was removed from the thoracic cavity by gentle chest compression. For remaining organs, the skin was denuded (VEET; Rickett Benckiser, Berkshire, UK) and sterilized above the abdomen (liver and pancreas), left flank (kidney), and upper hind limb (skeletal muscle). The respective organ was exposed, two 15 μL (15 or 25 μg; see Figure 2) injections were administered, and the skin was closed by suturing.

Assessment of Luciferase Protein Expression following Direct Tissue Injection

At the predetermined time points following injection, male NMRI mice (10–12 weeks old) or female BALB/c 16–20 weeks old) were anesthetized with 2%–3% isoflurane. A 150 mg/kg aqueous solution of D-Luciferin (XenoLight D-luciferin K^+ Salt; Perkins Elmer, Waltham, MA, USA) was given via intra-peritoneal injection. After 15 min, IVIS spectrum imaging was performed on the IVIS system (Xenogen, Alameda, CA, USA) and analyzed with Living Image software (Xenogen). During image acquisition, isoflurane anesthesia was maintained using nose cone delivery system, and animal body temperature was regulated using a digital thermostat bed integrated within the IVIS system. To evaluate extra cardiac or skeletal muscle expression, the animal was given another intraperitoneal injection of D-Luciferin, and after 15 min the animal was sacrificed while under anesthesia. The heart or quadriceps muscle was then exposed. IVIS exposure time was increased to 5 min, and the image was acquired.

Assessment of β-Galactosidase Protein following Single Intracardiac Injection of *lacZ* mRNA in the Mouse

Forty-eight hours after citrate-saline buffered *lacz* mRNA cardiac injection, the heart was excised, briefly rinsed in phosphate buffer and fixated in 4% paraformaldehyde for 15 min, and then washed three times (20–30 min) with 0.1 mmol/L phosphate (pH 7.3) wash buffer containing 2 mmol/L $MgCl_2$, 0.01% sodium deoxycholate, and 0.02% Nonidet P-40. Subsequently, freshly prepared X-gal solution [phosphate wash buffer containing 5 mmol/L $K_4Fe(CN)_6$, 5 mmol/L $K_3Fe/CN)_6$ and 1 mg/mL X-gal] was added to the specimen, which then was wrapped in foil and incubated at 37°C overnight. The specimen was then washed with phosphate wash buffer three times and photographed.

In Situ Hybridization for *VEGF* mRNA and Immunohistochemistry for VEGF-A Protein in Cardiac Tissue

Male Sprague-Dawley rats were anesthetized with isoflurane, and the left thoracic region was shaved and sterilized following intubation.

The thoracic region was injected with Marcaine subcutaneously (25 mg/kg) and buprenorphine (0.05 mg/kg) for analgesia. The heart was exposed through a left thoracotomy at the fifth intercostal space. *VEGF* mRNA (100 μg) formulated in citrate-saline was injected as three separate injections (20 μL each, total volume 60 μL) along a line in the left ventricular free wall. Separate animals were injected with citrate-saline (three separate injections of 20 μL each, total volume 60 μL). After the injection, the thorax and the skin were closed by suturing, and excess air was removed from the thoracic cavity by gentle chest compression. Subsequently, when normal breathing was established, the rat was disconnected from the ventilator and brought back to its home cage. At predefined time points (1, 3, 6, 24, 48, 72, 192 hr) following the cardiac injection, the rat was anesthetized and the chest opened a second time for heart tissue sampling. Animals injected with citrate-saline were terminated, and tissue was harvested 3 and 72 hr after the injection. The heart was excised and the right ventricle trimmed off, and the left ventricle was put in 4% formaldehyde for fixation.

Excised hearts were fixated in formaldehyde, and transversely sliced at the injection site and 2 mm distally in both directions. Subsequently, the slices were embedded in paraffin further sectioned into 4-μm slices. RNAscope automated *in situ* hybridization assay for detection of *VEGF* mRNA was carried out in the Bond RX platform (Leica Biosystems, Wetzlar, Germany), and all *in situ* hybridization reagents were ACD products (Advanced Cell Diagnostics, Newark, CA, USA). In brief, target retrieval was performed at 95°C for 15 min using Leica Epitope Retrieval Buffer 2 followed by protease treatment at 42°C for 15 min. The probe (RNA scope LS2.5 Probe-Hs-VEGFA-noXrodent cat. No. 412018; ACD) was hybridized for 2 hr at 42°C followed by RNA scope amplification, and 3,3′-diaminobenzidine (DAB) was used for visualization of staining. As positive and negative controls, RNAscope 2.5 LS probe-Rn-Ppib and RNAscope 2.5 LS Negative Control Probe_dapB were used. Immunohistochemistry for detection of VEGF-A protein, troponin T, and dual immunohistochemistry VEGF-A/troponin T was carried out in the Ventana discovery Ultra immunostainer according to manufacturer's recommendation, and all reagents were Ventana products (Roche, Basel, Switzerland). Antigen retrieval was done in Ventana Cell Conditioner 1 at 95°C. Primary antibodies (anti-rabbit hVEGF-A, dilution 1:100, cat. No. RB-9031-P0 [Thermo Scientific, Waltham, MA, USA]; anti-mouse troponin T, dilution 1:400, cat. No. MS-295-P1 [Thermo Scientific]) were added for 1 hr at 37°C followed by secondary anti-rabbit HQ or secondary anti-mouse nitropyrazole (NP). For enhancement of the staining, anti-HQ horseradish peroxidase (HRP) or anti-NP/alkaline phosphatase (AP) was used and detected with Purple- or Yellow chromogenic detection kit.

Assessment of Human VEGF-A Protein Production following Intracardiac Injection of *VEGF* mRNA in the Rat

As described above, rats were intracardially injected with purified *VEGF* mRNA (1800, 150, or 15 μg as six separate injections, 15 μL each) along a line in the left ventricular free wall. At predefined time points following the cardiac injections, the rat was anesthetized and the chest opened. The heart was excised and the right ventricle and the atria trimmed off. A transverse slice from the left ventricular free wall including the injection sites was excised, divided in two parts that were snap frozen in liquid nitrogen, and stored at −80°C until analysis of human VEGF-A protein as described above.

Quantification of Human VEGF-A Protein in Cardiac Tissue

Tris lysis buffer containing phosphatase inhibitors I and II and protease inhibitor (Meso Scale Discovery [MSD], Rockville, MD, USA) was added to the frozen tissue biopsies and frozen at approximately −20°C prior to homogenization. Ceramic beads (3 mm) were added and the samples homogenized using the Precellys homogenizer instrument. The homogenates were centrifuged and the supernatants stored at −80°C prior to analysis. VEGF-A concentrations were determined using a sandwich immunoassay with electrochemical luminescent detection. MSD V-PLEX cytokine Panel 1 (human) VEGF-A kits were used to measure the VEGF-A concentration in the tissue homogenates as per the kit instructions. The plates were read on the MSD Sector 600 instrument.

Measurement of Left Ventricular Function and IS following Intracardiac Injection of *VEGF* mRNA in Rats

Rats were anesthetized, pretreated, thoracotomized, and underwent LAD ligation as described above. The ligation was followed by six intracardiac injections (90 μL in total) of either vehicle (citrate-saline), 150, or 1,800 μg purified *VEGF* mRNA along the border zone. On the day following the surgical procedure, a blood sample was drawn from the tail vein for analysis of cardiac troponin I (i-STAT cardiac troponin I diagnostic test; Abbott Point of Care, Abbott Park, IL, USA).

At 1 and at 8 days after surgery, left ventricular function and ISs were assessed via magnetic resonance imaging (MRI) using a 4.7T small-animal scanner (Bruker Biospin, Ettlingen, Germany). End-diastolic volumes (EDVs) and end-systolic volumes (ESVs) were evaluated from short-axis images covering the left ventricle (prospectively triggered gradient-echo sequence) via manual delineation of the endocardium in end-diastole and end-systole using the software package Segment (Medviso AB, Lund, Sweden). Ejection fraction (EF) was calculated as (EDV − ESV)/EDV. Infarcted myocardium was visualized in late-Gadolinium enhancement scans (inversion-recovery gradient-echo sequence) covering the left ventricle. The images were acquired 10 min after the administration of 0.3 mmol/kg Gadodiamide (GE Healthcare, Chicago, IL, USA) via a tail-vein catheter. The left ventricle wall volumes and the infarct volumes were manually delineated, and the IS was determined as the infarct volume fraction of the left ventricular wall.

Assessment of Human VEGF-A Protein following Intracardiac Injection of *VEGF* mRNA in Mini Pigs

All experiments were carried out according to European Community Council Directives and approved by the Göteborgs Djurförsöksetiska Nämnd (Göteborg, Sweden). Female Göttingen mini pigs (body weight ∼25 kg) fasted overnight were sedated through an

intramuscular injection of midazolam and ketamine. Following sedation, the pig was intubated, and general anesthesia was maintained by isoflurane. A left thoracotomy to expose the heart was carried out, and purified *VEGF* mRNA in citrate-saline was injected in the left ventricular free wall at a depth approximately 5 mm from the epicardial surface. The injection site was marked with a small suture, and 6 hr later the heart was excised. Transmural tissue slabs were harvested at the injection sites. For human VEGF-A protein analysis, each tissue slab was divided in six separate specimens from epicardium to endocardium. These specimens were snap frozen in liquid nitrogen and stored at −80°C until human VEGF-A analysis as described above.

Effects on Left Ventricular Function, IS, Capillary and Arteriole Density, and Fibrosis following Intracardiac Injection of *VEGF* mRNA in Mini Pigs Subjected to Myocardial Infarction

The animal experiments were carried out at the National Laboratory Animal Centre (Tainan, Taiwan), an Association for Assessment and Accreditation of Laboratory Animal Care International (AAALAC)-accredited facility. All animal research procedures were approved in accordance to IACUC guidelines. Female, sexually mature, Lanyu mini pigs (~5 months old, 20 ± 2.1 kg) obtained from the National Taitung Animal Propagation Station (Taitung, Taiwan) were used for this study. Prior to each surgery, animals were fasted overnight and then anaesthetized with Zoletil (4 mg/kg; Vibrac, France) and Xylazine (2.2 mg/kg; Bayer, Korea) by intramuscular injection, in conjunction with buprenorphine (0.05 mg/kg; O-Smart, Taiwan) subcutaneously. Upon endotracheal intubation and attachment to a respirator (Dräger AG & CO, Lubeck, Germany), a mixture of oxygen, air, and isoflurane (0.4%–2%; Panion & BF, Taiwan) was supplied. Saline, anesthetic, and emergency drugs were supplied intravenously via an indwelling needle in an ear vein, if necessary. Vital signs (heart rate, blood pressure, respiration rate, O_2 pulse oximeter, ECG, and body temperature) were continuously monitored throughout each surgical procedure. Upon conclusion of each procedure, animals were transitioned to an intensive care unit for approximately 2 hr before being returned to the pen. Analgesics and antibiotics were administered to relieve pain and prevent infection before and after surgeries.

Induction of MI and Delivery of Study Drugs

A total of 29 mini pigs were used for the study. Animals were randomly divided into four blinded groups: sham (n = 5), vehicle (citrate-saline, n = 8), purified VEGF mRNA low dose (1 mg, n = 8) or purified *VEGF* mRNA high dose (10 mg, n = 8). After preparation of animals as above, a left thoracotomy was performed to expose the heart. To induce injury, we permanently ligated the mid-left anterior descending coronary artery in all pigs except the sham group. Subsequently, the chest was closed and animals were sent to the intensive care unit until fit to be returned to the pen as above. Seven days after the initial surgery, the animals were subjected to a second thoracotomy through the same incision wound. The study drugs were then administered equally to the infarct and peri-infarct area via intracardiac injection (~20 delivery sites, 100 μL/site, 26G needle). After the procedure, the pigs were handled as described above and left to recover for 2 months before sacrifice.

Echocardiography

Heart function was assessed by 2D echocardiography using Vivid Q with a 3.6-MHz probe (GE Healthcare, Horten, Norway) immediately before and after induction of MI, immediately before drug delivery (7 days after ligation), and then on the day of sacrifice 2 months after treatment. Measurements were taken under anesthesia in the closed-chest setting and the pigs placed in the left lateral decubitus position. Parasternal long-axis views were obtained by M mode to measure left ventricular volumes to derive LVEF.

Invasive Hemodynamics

After the final echocardiography recording and prior to sacrifice, measurement of hemodynamics was performed using a PV loop recording catheter (Millar Instruments, Houston, TX, USA). Labchart 8 (AD Instruments) was used to direct the process and analyze data. Two milliliters of blood was drawn to calibrate conductance for volume conversion. Upon stabilization of the catheter, which was inserted into the left ventricular cavity via the carotid artery, baseline LV PV loops were recorded. Preload was reduced by transiently clamping the inferior vena cava through an incision in the upper abdomen. To determine parallel conductance, we injected 10 mL of 25% saline through the right jugular vein.

Infarct Area and Length

Upon completion of hemodynamic assessment, the pig was sacrificed and the heart was harvested, washed three times, and processed into five slices from the apex to the papillary muscle level. It has previously been shown that this is the optimal method for representing the entire infarction.[59] Images were taken of each slice, and the ISs were calculated using computer software (ImageJ). Infarct area was calculated as a percentage of the area of the whole ventricle minus the area of the inner space. Infarct length was calculated as the percentage of the midline circumference of the ventricular chamber of each slice. Regions where the injury was less than half the width of the ventricular wall were not considered for infarct length calculations.

Angiogenesis and Arteriogenesis Assay

Samples from the peri-infarct area were fixed in 4% paraformaldehyde at 4°C for at least 24 hr and then paraffin embedded. Following sectioning, deparaffinization, and rehydration, antigen retrieval was performed by boiling in 10 mmol/L sodium citrate buffer (pH 6; Sigma-Aldrich) for 10 min. Sections were then incubated with anti-cardiac troponin I (1:200; Developmental Studies Hybridoma Bank, Iowa City, IA, USA), anti-isolectin (1:100; Invitrogen), and SM-22α (1:200; Abcam, Cambridge, UK) overnight. After washing three times, sections were then incubated with the relevant Alexa Fluor 488 or 568 antibodies (Invitrogen). Nuclei were stained with DAPI (Sigma-Aldrich). After mounting, capillary and arteriole densities were calculated by manually counting and averaging from images (×200 magnification) taken at three randomly selected areas along the peri-infarct region.

Fibrosis Measurement

Samples from the remote area were processed as above for peri-infarct area samples. Fibrosis, as a function of collagen deposition, was determined using Masson's trichrome. Images from three randomly selected areas were taken using bright-field microscopy (×200 magnification) for each section and then quantified (AxioVision; Zeiss) and averaged.

Statistical Analysis

All measurements are presented as means ± SEM. Statistical significance was calculated using one-way or two-way ANOVA followed by either Tukey's multiple comparison test when comparing different treatments and time points or Dunnett's multiple comparison test when comparing to vehicle control at a specific time point. All groups displayed normal distributions and consistent variance. The p values <0.05 were considered statistically significant. Power calculations were not performed to determine sample size. There were no pre-specific inclusion or exclusion criteria. All animals were randomized to treatment. No animals were excluded from the small-animal cohorts. From the large-animal studies, some exclusions were made based on anomalous recovery (complete lack of infarct) or for technical reasons. Investigators were blinded to *VEGF* mRNA post-MI treatments and outcome assessments.

SUPPLEMENTAL INFORMATION

Supplemental Information includes Supplemental Materials and Methods, one figure, and four tables and can be found with this article online at https://doi.org/10.1016/j.omtm.2018.04.003.

AUTHOR CONTRIBUTIONS

L.C., J.C.C., P.C.H.H., K.R.C., and R.F.-D. conceived and designed the experiments. L.C., J.C.C., and C.Y. prepared the figures and wrote the manuscript. J.C.C., C.Y., T.A., M.B., A.-C.E., K.J., E.J., G.L., S.M., M.W.S., N.W., C.-H.C., Y.-P.W., and S.L. performed the experiments. L.C., J.C.C., C.Y., F.G., L.-M.G., B.T., Q.-D.W., P.C.H.H., K.R.C., and R.F.-D. analyzed the data and reviewed the manuscript.

CONFLICTS OF INTEREST

L.C., T.A., A.-C.E., L.-M.G., K.J., E.J., G.L., S.M., M.W.S., and Q.-D.W. are employees of AstraZeneca. F.G. and B.T. are employees of Moderna Therapeutics. K.R.C. and J.C.C. are advisors to AstraZeneca. K.R.C. is a co-founder of Moderna Therapeutics. There are three unpublished provisional applications directed to the subject matter of the paper.

ACKNOWLEDGMENTS

Kristine Bylund, Pedro Sousa, Madeleine Antonsson, Monika Sundqvist, Mikko Hölttä, Malin Palmér, Karen Woods, Alan Sabirsh, Katarina Rydén Markinhuhta, and Kristine Burke are greatly acknowledged for technical support and advice. We thank the National Laboratory Animal Center, Tainan, Taiwan, for technical assistance with pig experiments. P.C.H.H. receives research grants from AstraZeneca and Takeda.

REFERENCES

1. Selvin, E., Marinopoulos, S., Berkenblit, G., Rami, T., Brancati, F.L., Powe, N.R., and Golden, S.H. (2004). Meta-analysis: glycosylated hemoglobin and cardiovascular disease in diabetes mellitus. Ann. Intern. Med. *141*, 421–431.
2. Criqui, M.H., and Aboyans, V. (2015). Epidemiology of peripheral artery disease. Circ. Res. *116*, 1509–1526.
3. Mozaffarian, D., Benjamin, E.J., Go, A.S., Arnett, D.K., Blaha, M.J., Cushman, M., de Ferranti, S., Després, J.P., Fullerton, H.J., Howard, V.J., et al.; American Heart Association Statistics Committee and Stroke Statistics Subcommittee (2015). Heart disease and stroke statistics—2015 update: a report from the American Heart Association. Circulation *131*, e29–e322.
4. Henry, T.D., Annex, B.H., McKendall, G.R., Azrin, M.A., Lopez, J.J., Giordano, F.J., Shah, P.K., Willerson, J.T., Benza, R.L., Berman, D.S., et al.; VIVA Investigators (2003). The VIVA trial: vascular endothelial growth factor in ischemia for vascular angiogenesis. Circulation *107*, 1359–1365.
5. Gyöngyösi, M., Khorsand, A., Zamini, S., Sperker, W., Strehblow, C., Kastrup, J., Jorgensen, E., Hesse, B., Tägil, K., Bøtker, H.E., et al. (2005). NOGA-guided analysis of regional myocardial perfusion abnormalities treated with intramyocardial injections of plasmid encoding vascular endothelial growth factor A-165 in patients with chronic myocardial ischemia: subanalysis of the EUROINJECT-ONE multicenter double-blind randomized study. Circulation *112* (*Suppl 9*), I157–I165.
6. Svitkin, Y.V., Cheng, Y.M., Chakraborty, T., Presnyak, V., John, M., and Sonenberg, N. (2017). N1-methyl-pseudouridine in mRNA enhances translation through eIF2α-dependent and independent mechanisms by increasing ribosome density. Nucleic Acids Res. *45*, 6023–6036.
7. Sultana, N., Magadum, A., Hadas, Y., Kondrat, J., Singh, N., Youssef, E., Calderon, D., Chepurko, E., Dubois, N., Hajjar, R.J., and Zangi, L. (2017). Optimizing cardiac delivery of modified mRNA. Mol. Ther. *25*, 1306–1315.
8. Richner, J.M., Himansu, S., Dowd, K.A., Butler, S.L., Salazar, V., Fox, J.M., Julander, J.G., Tang, W.W., Shresta, S., Pierson, T.C., et al. (2017). Modified mRNA vaccines protect against Zika virus infection. Cell *168*, 1114–1125.e10.
9. Ferrara, N., Gerber, H.-P., and LeCouter, J. (2003). The biology of VEGF and its receptors. Nat. Med. *9*, 669–676.
10. Lui, K.O., Zangi, L., Silva, E.A., Bu, L., Sahara, M., Li, R.A., Mooney, D.J., and Chien, K.R. (2013). Driving vascular endothelial cell fate of human multipotent Isl1+ heart progenitors with VEGF modified mRNA. Cell Res. *23*, 1172–1186.
11. Zangi, L., Lui, K.O., von Gise, A., Ma, Q., Ebina, W., Ptaszek, L.M., Später, D., Xu, H., Tabebordbar, M., Gorbatov, R., et al. (2013). Modified mRNA directs the fate of heart progenitor cells and induces vascular regeneration after myocardial infarction. Nat. Biotechnol. *31*, 898–907.
12. Annex, B.H. (2013). Therapeutic angiogenesis for critical limb ischaemia. Nat. Rev. Cardiol. *10*, 387–396.
13. Isner, J.M., Pieczek, A., Schainfeld, R., Blair, R., Haley, L., Asahara, T., Rosenfield, K., Razvi, S., Walsh, K., and Symes, J.F. (1996). Clinical evidence of angiogenesis after arterial gene transfer of phVEGF165 in patient with ischaemic limb. Lancet *348*, 370–374.
14. Vale, P.R., Losordo, D.W., Milliken, C.E., McDonald, M.C., Gravelin, L.M., Curry, C.M., Esakof, D.D., Maysky, M., Symes, J.F., and Isner, J.M. (2001). Randomized, single-blind, placebo-controlled pilot study of catheter-based myocardial gene transfer for therapeutic angiogenesis using left ventricular electromechanical mapping in patients with chronic myocardial ischemia. Circulation *103*, 2138–2143.
15. Losordo, D.W., Vale, P.R., Hendel, R.C., Milliken, C.E., Fortuin, F.D., Cummings, N., Schatz, R.A., Asahara, T., Isner, J.M., and Kuntz, R.E. (2002). Phase 1/2 placebo-controlled, double-blind, dose-escalating trial of myocardial vascular endothelial growth factor 2 gene transfer by catheter delivery in patients with chronic myocardial ischemia. Circulation *105*, 2012–2018.
16. Kastrup, J., Jørgensen, E., Rück, A., Tägil, K., Glogar, D., Ruzyllo, W., Bøtker, H.E., Dudek, D., Drvota, V., Hesse, B., et al.; Euroinject One Group (2005). Direct intramyocardial plasmid vascular endothelial growth factor-A165 gene therapy in patients with stable severe angina pectoris: a randomized double-blind placebo-controlled study: the Euroinject One trial. J. Am. Coll. Cardiol. *45*, 982–988.
17. Favaloro, L., Diez, M., Mendiz, O., Janavel, G.V., Valdivieso, L., Ratto, R., Garelli, G., Salmo, F., Criscuolo, M., Bercovich, A., and Crottogini, A. (2013). High-dose

plasmid-mediated VEGF gene transfer is safe in patients with severe ischemic heart disease (Genesis-I). A phase I, open-label, two-year follow-up trial. Catheter. Cardiovasc. Interv. *82*, 899–906.

18. Tio, R.A., Tkebuchava, T., Scheuermann, T.H., Lebherz, C., Magner, M., Kearny, M., Esakof, D.D., Isner, J.M., and Symes, J.F. (1999). Intramyocardial gene therapy with naked DNA encoding vascular endothelial growth factor improves collateral flow to ischemic myocardium. Hum. Gene Ther. *10*, 2953–2960.

19. Rudin, C.M., Marshall, J.L., Huang, C.H., Kindler, H.L., Zhang, C., Kumar, D., Gokhale, P.C., Steinberg, J., Wanaski, S., Kasid, U.N., and Ratain, M.J. (2004). Delivery of a liposomal c-raf-1 antisense oligonucleotide by weekly bolus dosing in patients with advanced solid tumors: a phase I study. Clin. Cancer Res. *10*, 7244–7251.

20. Coelho, T., Adams, D., Silva, A., Lozeron, P., Hawkins, P.N., Mant, T., Perez, J., Chiesa, J., Warrington, S., Tranter, E., et al. (2013). Safety and efficacy of RNAi therapy for transthyretin amyloidosis. N. Engl. J. Med. *369*, 819–829.

21. Pollard, C., Rejman, J., De Haes, W., Verrier, B., Van Gulck, E., Naessens, T., De Smedt, S., Bogaert, P., Grooten, J., Vanham, G., and De Koker, S. (2013). Type I IFN counteracts the induction of antigen-specific immune responses by lipid-based delivery of mRNA vaccines. Mol. Ther. *21*, 251–259.

22. Carlsson, L., Yen, C.Y., Wang, Y.P., Lin, R.H., and Lo, A.H. (2016). A biocompatible chemically modified mRNA drives sustained VEGF-A protein production, human endothelial angiogenesis and epicardial progenitor expansion, and reduces infarct size and partially reverses global cardiac dysfunction when intracardially injected one week post-myocardial infarction in the pig. Circulation *134*, A15533.

23. Cantara, W.A., Crain, P.F., Rozenski, J., McCloskey, J.A., Harris, K.A., Zhang, X., Vendeix, F.A., Fabris, D., and Agris, P.F. (2011). The RNA Modification Database, RNAMDB: 2011 update. Nucleic Acids Res. *39*, D195–D201.

24. Gehrig, S., Eberle, M.E., Botschen, F., Rimbach, K., Eberle, F., Eigenbrod, T., Kaiser, S., Holmes, W.M., Erdmann, V.A., Sprinzl, M., et al. (2012). Identification of modifications in microbial, native tRNA that suppress immunostimulatory activity. J. Exp. Med. *209*, 225–233.

25. Sampson, J.R., and Uhlenbeck, O.C. (1988). Biochemical and physical characterization of an unmodified yeast phenylalanine transfer RNA transcribed in vitro. Proc. Natl. Acad. Sci. USA *85*, 1033–1037.

26. Helm, M. (2006). Post-transcriptional nucleotide modification and alternative folding of RNA. Nucleic Acids Res. *34*, 721–733.

27. Anderson, B.R., Muramatsu, H., Nallagatla, S.R., Bevilacqua, P.C., Sansing, L.H., Weissman, D., and Karikó, K. (2010). Incorporation of pseudouridine into mRNA enhances translation by diminishing PKR activation. Nucleic Acids Res. *38*, 5884–5892.

28. Karikó, K., Muramatsu, H., Keller, J.M., and Weissman, D. (2012). Increased erythropoiesis in mice injected with submicrogram quantities of pseudouridine-containing mRNA encoding erythropoietin. Mol. Ther. *20*, 948–953.

29. Wolff, J.A., Malone, R.W., Williams, P., Chong, W., Acsadi, G., Jani, A., and Felgner, P.L. (1990). Direct gene transfer into mouse muscle in vivo. Science *247*, 1465–1468.

30. Jirikowski, G.F., Sanna, P.P., Maciejewski-Lenoir, D., and Bloom, F.E. (1992). Reversal of diabetes insipidus in Brattleboro rats: intrahypothalamic injection of vasopressin mRNA. Science *255*, 996–998.

31. Karikó, K., Muramatsu, H., Ludwig, J., and Weissman, D. (2011). Generating the optimal mRNA for therapy: HPLC purification eliminates immune activation and improves translation of nucleoside-modified, protein-encoding mRNA. Nucleic Acids Res. *39*, e142.

32. Sander, L.E., Davis, M.J., Boekschoten, M.V., Amsen, D., Dascher, C.C., Ryffel, B., Swanson, J.A., Müller, M., and Blander, J.M. (2011). Detection of prokaryotic mRNA signifies microbial viability and promotes immunity. Nature *474*, 385–389.

33. Karikó, K., Muramatsu, H., Welsh, F.A., Ludwig, J., Kato, H., Akira, S., and Weissman, D. (2008). Incorporation of pseudouridine into mRNA yields superior nonimmunogenic vector with increased translational capacity and biological stability. Mol. Ther. *16*, 1833–1840.

34. Karikó, K., Ni, H., Capodici, J., Lamphier, M., and Weissman, D. (2004). mRNA is an endogenous ligand for Toll-like receptor 3. J. Biol. Chem. *279*, 12542–12550.

35. Anderson, B.R., Muramatsu, H., Jha, B.K., Silverman, R.H., Weissman, D., and Karikó, K. (2011). Nucleoside modifications in RNA limit activation of 2′-5′-oligoadenylate synthetase and increase resistance to cleavage by RNase L. Nucleic Acids Res. *39*, 9329–9338.

36. Karikó, K., Buckstein, M., Ni, H., and Weissman, D. (2005). Suppression of RNA recognition by Toll-like receptors: the impact of nucleoside modification and the evolutionary origin of RNA. Immunity *23*, 165–175.

37. Heil, F., Hemmi, H., Hochrein, H., Ampenberger, F., Kirschning, C., Akira, S., Lipford, G., Wagner, H., and Bauer, S. (2004). Species-specific recognition of single-stranded RNA via toll-like receptor 7 and 8. Science *303*, 1526–1529.

38. Züst, R., Cervantes-Barragan, L., Habjan, M., Maier, R., Neuman, B.W., Ziebuhr, J., Szretter, K.J., Baker, S.C., Barchet, W., Diamond, M.S., et al. (2011). Ribose 2′-O-methylation provides a molecular signature for the distinction of self and non-self mRNA dependent on the RNA sensor Mda5. Nat. Immunol. *12*, 137–143.

39. Probst, J., Weide, B., Scheel, B., Pichler, B.J., Hoerr, I., Rammensee, H.G., and Pascolo, S. (2007). Spontaneous cellular uptake of exogenous messenger RNA in vivo is nucleic acid-specific, saturable and ion dependent. Gene Ther. *14*, 1175–1180.

40. Kormann, M.S.D., Hasenpusch, G., Aneja, M.K., Nica, G., Flemmer, A.W., Herber-Jonat, S., Huppmann, M., Mays, L.E., Illenyi, M., Schams, A., et al. (2011). Expression of therapeutic proteins after delivery of chemically modified mRNA in mice. Nat. Biotechnol. *29*, 154–157.

41. Chen, C.-H., Chang, M.-Y., Wang, S.-S., and Hsieh, P.C.H. (2014). Injection of autologous bone marrow cells in hyaluronan hydrogel improves cardiac performance after infarction in pigs. Am. J. Physiol. Heart Circ. Physiol. *306*, H1078–H1086.

42. Lin, Y.-D., Yeh, M.L., Yang, Y.J., Tsai, D.C., Chu, T.Y., Shih, Y.Y., Chang, M.Y., Liu, Y.W., Tang, A.C., Chen, T.Y., et al. (2010). Intramyocardial peptide nanofiber injection improves postinfarction ventricular remodeling and efficacy of bone marrow cell therapy in pigs. Circulation *122* (*Suppl 11*), S132–S141.

43. Lin, Y.-D., Luo, C.Y., Hu, Y.N., Yeh, M.L., Hsueh, Y.C., Chang, M.Y., Tsai, D.C., Wang, J.N., Tang, M.J., Wei, E.I., et al. (2012). Instructive nanofiber scaffolds with VEGF create a microenvironment for arteriogenesis and cardiac repair. Sci. Transl. Med. *4*, 146ra109.

44. Sharp, T.E., 3rd, Schena, G.J., Hobby, A.R., Starosta, T., Berretta, R.M., Wallner, M., Borghetti, G., Gross, P., Yu, D., Johnson, J., et al. (2017). Cortical Bone Stem Cell Therapy Preserves Cardiac Structure and Function After Myocardial Infarction. Circ. Res. *121*, 1263–1278.

45. Schwarz, E.R., Speakman, M.T., Patterson, M., Hale, S.S., Isner, J.M., Kedes, L.H., and Kloner, R.A. (2000). Evaluation of the effects of intramyocardial injection of DNA expressing vascular endothelial growth factor (VEGF) in a myocardial infarction model in the rat—angiogenesis and angioma formation. J. Am. Coll. Cardiol. *35*, 1323–1330.

46. Eppler, S.M., Combs, D.L., Henry, T.D., Lopez, J.J., Ellis, S.G., Yi, J.H., Annex, B.H., McCluskey, E.R., and Zioncheck, T.F. (2002). A target-mediated model to describe the pharmacokinetics and hemodynamic effects of recombinant human vascular endothelial growth factor in humans. Clin. Pharmacol. Ther. *72*, 20–32.

47. Gerber, H.P., Dixit, V., and Ferrara, N. (1998). Vascular endothelial growth factor induces expression of the antiapoptotic proteins Bcl-2 and A1 in vascular endothelial cells. J. Biol. Chem. *273*, 13313–13316.

48. Huang, P.L. (2009). eNOS, metabolic syndrome and cardiovascular disease. Trends Endocrinol. Metab. *20*, 295–302.

49. Dvorak, H.F., Brown, L.F., Detmar, M., and Dvorak, A.M. (1995). Vascular permeability factor/vascular endothelial growth factor, microvascular hyperpermeability, and angiogenesis. Am. J. Pathol. *146*, 1029–1039.

50. Folkman, J., Merler, E., Abernathy, C., and Williams, G. (1971). Isolation of a tumor factor responsible for angiogenesis. J. Exp. Med. *133*, 275–288.

51. Carmeliet, P., and Jain, R.K. (2000). Angiogenesis in cancer and other diseases. Nature *407*, 249–257.

52. Simons, M., and Eichmann, A. (2015). Molecular controls of arterial morphogenesis. Circ. Res. *116*, 1712–1724.

53. Bernatchez, P.N., Soker, S., and Sirois, M.G. (1999). Vascular endothelial growth factor effect on endothelial cell proliferation, migration, and platelet-activating factor synthesis is Flk-1-dependent. J. Biol. Chem. *274*, 31047–31054.

54. Vasudev, N.S., and Reynolds, A.R. (2014). Anti-angiogenic therapy for cancer: current progress, unresolved questions and future directions. Angiogenesis *17*, 471–494.

55. Lai, K., and Landa, G. (2015). Current choice of treatments for neovascular AMD. Expert Rev. Clin. Pharmacol. *8*, 135–140.

56. Kaczmarek, J.C., Kowalski, P.S., and Anderson, D.G. (2017). Advances in the delivery of RNA therapeutics: from concept to clinical reality. Genome Med. *9*, 60.

57. Lorenz, C., Fotin-Mleczek, M., Roth, G., Becker, C., Dam, T.C., Verdurmen, W.P., Brock, R., Probst, J., and Schlake, T. (2011). Protein expression from exogenous mRNA: uptake by receptor-mediated endocytosis and trafficking via the lysosomal pathway. RNA Biol. *8*, 627–636.

58. Xue, H.Y., Liu, S., and Wong, H.L. (2014). Nanotoxicity: a key obstacle to clinical translation of siRNA-based nanomedicine. Nanomedicine (Lond.) *9*, 295–312.

59. Takagawa, J., Zhang, Y., Wong, M.L., Sievers, R.E., Kapasi, N.K., Wang, Y., Yeghiazarians, Y., Lee, R.J., Grossman, W., and Springer, M.L. (2007). Myocardial infarct size measurement in the mouse chronic infarction model: comparison of area- and length-based approaches. J. Appl. Physiol. *102*, 2104–2111.